
Comparison of a novel coupled hydro-mechanical model with typical analytical models in subsidence of coal seam gas extraction

Guojun Wu

State Key Laboratory of Geomechanics and Geotechnical Engineering,
Institute of Rock and Soil Mechanics,
Chinese Academy of Sciences,
Bayi Road, Wuhan 430071, Hubei, China
Email: gjwu@whrsm.ac.cn

Shanpo Jia*

Research Center of Geomechanics and Geotechnical Engineering,
Yangtze University,
Nanhuan Road, Jingzhou 434023, Hubei, China
Email: jiashanporsm@163.com
*Corresponding author

Bailin Wu

CSIRO Energy,
71 Normanby Road,
Clayton, Melbourne 3168, Australia
Email: bailin.wu@csiro.au

Abstract: Although the influence of conventional oil and gas extraction on surface subsidence has been widely recognised and studied, few studies are carried out on the surface subsidence in coal seam gas fields and its impact on surface infrastructure and the environment. In predicting land subsidence caused by coal seam gas extraction, the hydro-mechanical behaviour of geological strata are different and their hydraulic connections to the coal seams are not well-understood, which makes the analytical models are difficult to be applied in the prediction of land subsidence. This paper develops a coupled fluid flow-geomechanical model which can consider the interrelation of fluid flow and geomechanics of the ground. By comparison of dewatering and degassing with typical analytical models including the disc-shaped reservoir model and the uniaxial compaction model, the typical analytical models cannot estimate the potential pressure distribution and predict the real subsidence induced by coal seam gas extraction; however, the coupled fluid flow-geomechanical model is capable of describing the transport properties of coal seam, including water flow, gas flow and desorption and rock deformation. Therefore, the proposed coupled model can be better used in analysis of subsidence of coal seam gas extraction. [Received: April 15, 2017; Accepted: October 17, 2017]

Keywords: land subsidence; depressurisation; gas extraction; analytical model; coal seam.

Reference to this paper should be made as follows: Wu, G., Jia, S. and Wu, B. (xxxx) ‘Comparison of a novel coupled hydro-mechanical model with typical analytical models in subsidence of coal seam gas extraction’, *Int. J. Oil, Gas and Coal Technology*, Vol. X, No. Y, pp.xxx–xxx.

Biographical notes: Guojun Wu received his PhD in Geotechnical Engineering from the University of Chinese Academy of Sciences. He is a researcher of State Key Laboratory of Geomechanics and Geotechnical Engineering at the Institute of Rock and Soil Mechanics, Chinese Academy of Sciences. His research interests include stability analysis of underground engineering and hydraulic fracturing.

Shanpo Jia received his Master’s in Petroleum Engineering from the China University of Petroleum in 2006, and his PhD in Geotechnical Engineering from the University of Chinese Academy of Sciences in 2009. He is a Professor of Research Center of Geomechanics and Geotechnical Engineering, Yangtze University. His current research interests include geofluid flow analysis, hydro-mechanical coupling of geomaterials and reservoir simulation.

Bailin Wu received his PhD in rock mechanics from the Imperial College London. He is a Senior Principal Research Scientist of the Commonwealth Scientific and Industrial Research Organisation (CSIRO), Australia. His research interests include stability analysis of sand production prediction, failure mechanisms and conceptualisation of hydrocarbon reservoir-aquifer failure pathways.

1 Introduction

Human activities for extracting natural resources, may lead to subsequent gradual or abrupt surface deformation, with adverse effects in the local ecosystem and damage to man-made structures (Moghaddam et al., 2016). Compared with the conventional gas production, mining or civil engineering activities, the subsidence caused by coal seam gas extraction is even more complicated due to the special interrelationship between the different phases (gas, liquid and solid) within coal seams. Land subsidence due to fluid (groundwater and gas) extraction occurs when the pore pressures in geologic unit decrease (Du and Olson, 2001; Gambolati et al., 2001). When groundwater and gas are extracted from coal seam formation, the reduction of pore pressure causes the compaction of different hydraulically connected geological units including the layers above and below the coal seams, due to the increase in effective vertical stress. This can result in subsidence of land surface. In addition, gas extraction from coal seam may result in additional compaction of the coal seams as gas desorption-induced shrinkage. The subsidence is the sum of these two processes and depends on each layer associated with the reduction of pore pressure (Chen et al., 2013; Zhu et al., 2007).

In predicting land subsidence, the main problem lies to the fact that the hydro-mechanical behaviour of each layer in geological profile is different and their hydraulic connection to the coal seams are not well-understood. Although a number of monitoring techniques to measure surface (tilt meter, levelling, GPS, InSAR) and sub-surface (extensometer, 4D seismic surveys) changes have emerged to detect the extent of the deformation and to quantify the rate of the deformation over extraction sites (Anderssohn

et al., 2009; Ramirez and Foxall, 2014; Sambridge, 1999a, 1999b; Vasco et al., 2009; Zhu et al., 2014), the expenses on the prediction of land subsidence are huge.

Under ideal conditions, if the hydro-mechanical behaviour of each layer can be acquired and the fluid flow in the coal is assumed as a single phase, it would be possible to predict the subsidence by the analytical method such as Geertsma's nucleus model and uniaxial compact model (Fjær et al., 2008; Geertsma, 1973). However, in reality, subsidence is difficult to predict by using the analytical methods due to the complex response of pore pressure of the entire geological profile to the gas extraction. The magnitude of subsidence mainly depends on the depth and thickness over which depressurisation and compaction occurs, and the properties of geological units overlying the compacting geological units. Numerical simulations for gas flow, mass transport and coupled gas-solid effect in coal seams have been widely applied (Basu et al., 1988; Wang and Peng, 2014; Zhu et al., 2007). Initially the coal seam is saturated with water, and thus the coalbed methane production begins with dewatering. The water-gas flow in coal seam can be described by Darcy's law and the gas diffusion in coal matrix is represented by Fick's law (Basu et al., 1988; Vandamme et al., 2010). These regimes occur in spatial sequence and progress outward from the well and into the coal seam. Two-phase flow occurs near the well, unsaturated water at some distance from the well and saturated water flow at greater distance from the well. The gas production is normally associated with a large amount of water, and thus a two-phase flow simulation is required to predict the water and gas production (Coussy et al., 2010). Subsidence associated with coal seam gas extraction can be predicted using numerical models that calculate the amount of depressurisation of various geological units and estimate the compact due to both changes in groundwater pressure and degassing of the coal seam.

In this study, a comparison of a novel coupled hydro-mechanical model with typical analytical models in subsidence of coal seam gas extraction is conducted. The results obtained from analytical solution are compared with those from numerical simulation for idealised condition, and then the superiority of the coupled model can be explained.

2 Typical analytical models of subsidence associated with CSG production

Presently, there are two typical analytical models, which are disc-shaped reservoir model and uniaxial compaction model.

2.1 Disc-shaped reservoir model

The surface deformation associated with gas extraction in a disc-shaped reservoir (Figure 1), can be calculated by the analytical solutions in the half space by Geertsma (1973). This approach is often used in the petroleum, and treats the reservoir as an inhomogeneous inclusion in a half space with the poroelasticity applied to the reservoir. Assuming that the overburden is uniform and elastic, the settlement and horizontal displacement in a surface point located at a distance from the gas well are given as follows:

$$\begin{cases} S(r, 0) = -\frac{C_m(1-\mu)}{\pi} \frac{D}{(r^2 + R^2)^{3/2}} \alpha \Delta p_f V \\ u_r(r, 0) = \frac{C_m(1-\mu)}{\pi} \frac{r}{(r^2 + R^2)^{3/2}} \alpha \Delta p_f V \end{cases} \quad (1)$$

where, C_m is the compressibility coefficient of rock, μ is the Poisson's ratio, r is the radial distance from vertical axis through the nucleus, R is the radius of disc-shaped reservoir, D is the depth of the reservoir, α is the Biot coefficient, Δp_f is the reservoir pressure changed value, and V is the volume of reservoir.

The compressibility coefficient C_m , which rock deformation is laterally constrained by, is related with the Young's modulus and Poisson's ratio. It can be defined as:

$$C_m = \frac{(1+\mu)(1-2\mu)}{E(1-\mu)} \quad (2)$$

For a fixed value of Young's modulus, C_m is changed with different Poisson's ratio. The calculated C_m values vary by less than 30% for Poisson's ratios between 0.1 and 0.3.

Given that such an idealised reservoir shape has been assumed, the reservoir pressure change Δp_f is suggested as a uniform reduction throughout the reservoir. The deformation above the disc-shaped reservoir can be integrated over the entire reservoir volume as follows:

$$\begin{cases} S(r, 0) = -2C_m(1-\mu)\alpha\Delta p_f HR \int_0^\infty e^{-Da} J_1(aR) J_0(ar) da \\ u_r(r, 0) = 2C_m(1-\mu)\alpha\Delta p_f HR \int_0^\infty e^{-Da} J_1(aR) J_1(ar) da \end{cases} \quad (3)$$

where S is the surface subsidence, u_r is the radial displacement, H is the thickness of reservoir, J_0 and J_1 are the Bessel function of zero and first order, respectively.

After the necessary mathematical manipulations, the more simple formulation can be obtained as follows:

$$\begin{cases} S(r, 0) = -2C_m(1-\mu)\alpha\Delta p_f HA(\rho, \eta) \\ u_r(r, 0) = 2C_m(1-\mu)\alpha\Delta p_f HB(\rho, \eta) \end{cases} \quad (4)$$

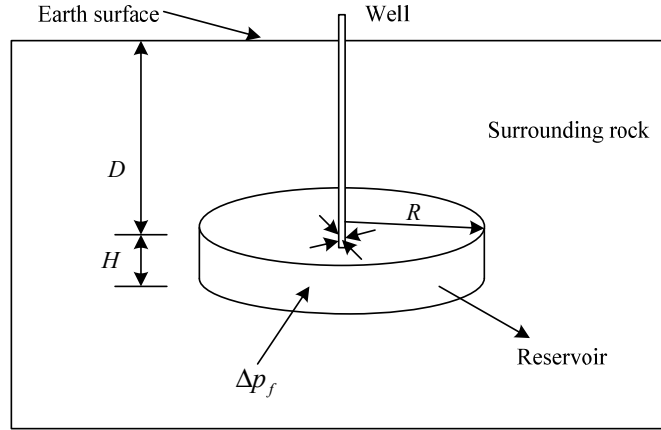
where C_m is the compressibility coefficient of rock, μ is the Poisson's ratio, r is the radial distance from vertical axis through the nucleus, α is the Biot coefficient, Δp_f is the changed value of reservoir pressure, $A(\rho, \eta)$ and $B(\rho, \eta)$ are the functions of the dimensionless ratios $\rho = r/R$ and $\eta = D/R$ (Fjær et al., 2008).

From equation (3), the gas extraction induced subsidence depends on three key parameters:

- 1 the compressibility coefficient C_m of coal seam
- 2 the Poisson's ratio
- 3 the poroelastic coefficient of the reservoir.

Geertsma's model is mainly limited to the case where there is no contrast in elastic properties between the reservoir and the surrounding layers and cannot consider the shrinkage effect associated with gas desorption of coal seam by depressurisation.

Figure 1 Reservoir configuration



2.2 Uniaxial compaction model

Assuming that the mechanical behaviour of the rock layer can be described by linear poroelasticity, the strain and stress of the target coal seam formation can be expressed by Hook's law, the normal strain in three dimensions can be written as Fjær et al. (2008):

$$\begin{cases} \varepsilon_x = \frac{1}{E} [\Delta\sigma'_x - \mu(\Delta\sigma'_y + \Delta\sigma'_z)] \\ \varepsilon_y = \frac{1}{E} [\Delta\sigma'_y - \mu(\Delta\sigma'_x + \Delta\sigma'_z)] \\ \varepsilon_z = \frac{1}{E} [\Delta\sigma'_z - \mu(\Delta\sigma'_x + \Delta\sigma'_y)] \end{cases} \quad (5)$$

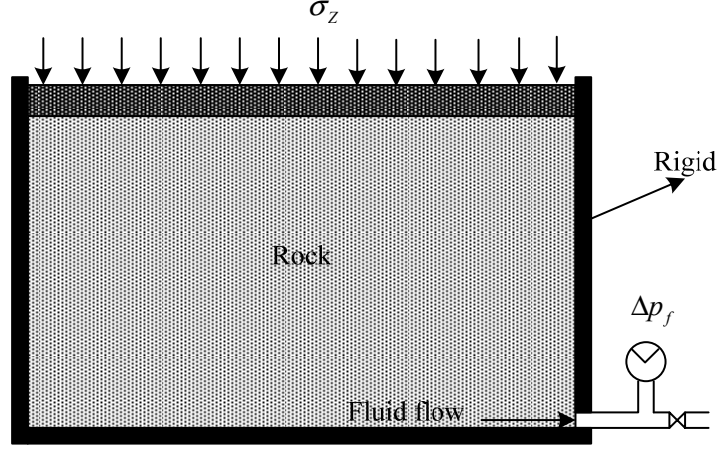
where σ' is the effective stress, ε is the strain, E and μ are the Young's modulus and Poisson's ratio of the target coal seam formation, respectively.

The rock layer is assumed to settle only in vertical direction and the lateral strain is neglected as only uniaxial deformation (Figure 2).

$$\varepsilon_x = \varepsilon_y = 0 \quad (6)$$

By inserting equation (6) into equation (5), the effective horizontal stresses can be written as:

$$\Delta\sigma'_x = \Delta\sigma'_y = \frac{\mu}{1-\mu} \Delta\sigma'_z \quad (7)$$

Figure 2 Uniaxial compaction model

The settlement of the target coal seam formation, S_{coal} , of thickness, H_{coal} , caused by the vertical strain, ε_z , can be written as follows:

$$\frac{S_{coal}}{H_{coal}} = \varepsilon_z = -\frac{1}{E} \frac{(1+\mu)(1-2\mu)}{(1-\mu)} \Delta\sigma'_z \quad (8)$$

According to the Biot theory, the pore pressure decreases and effective stress increases by fluid withdrawal in the example of CSG extraction. The effective vertical stress, $\Delta\sigma'_z$, can be written as :

$$\Delta\sigma'_z = \Delta\sigma_z - \alpha\Delta p_f \quad (9)$$

The total vertical stress, σ_z , is assumed to be constant stress during fluid withdrawal ($\Delta\sigma_z = 0$). The settlement can be defined as:

$$S_{coal} = C_m H_{coal} \alpha \Delta p_f \quad (10)$$

Land subsidence due to CSG extraction also results from two parts:

- a direct compact of coal seam formation
- b indirect compact of overlying and underlying geological units that are hydraulically connected to the coal seams.

The indirect compaction will be caused by the change in effective vertical stress or pore pressure within their own layers. The indirect compaction, $S_{indirect}$, can be defined as:

$$S_{indirect} = \sum_{i=1}^{N-1} C_{m(i)} H_{(i)} \alpha_{(i)} \Delta p_{f(i)} \quad (11)$$

where, $S_{indirect}$ is the indirect compaction of overlying and underlying geological strata, and N is the number of overlying and underlying geological units hydraulically connected to the target coal seam.

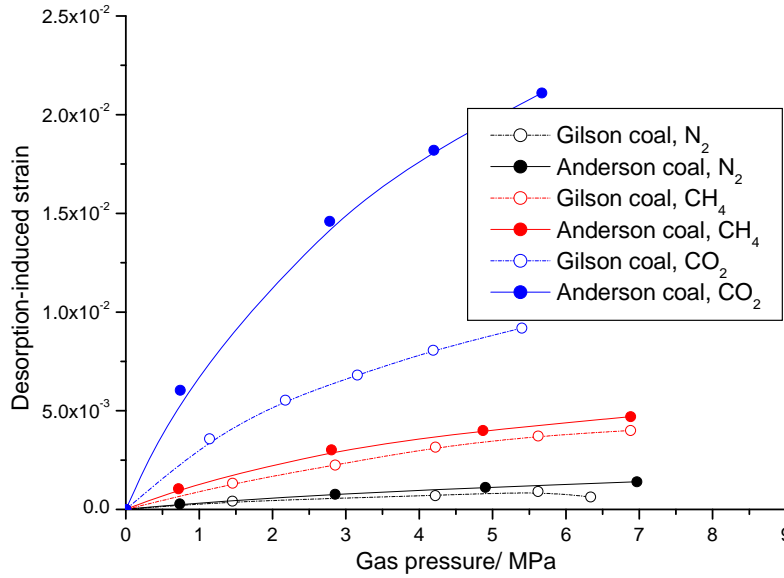
From the above, the target coal seam formation undergoes the compacting effect because of the pore pressure reduction of groundwater, which is determined by geomechanical compressibility, and similar to the other surrounding layers. Furthermore, desorption effect of coal seam degassing causes the additional compaction (shrinkage).

The desorption behaviour due to coal seam degassing conforms to the Langmuir isotherm (Wu et al., 2010; Zhang et al., 2008). Assuming that the target coal seam formation is constrained in the horizontal direction, the vertical compression of coal seam formation can be estimated by the Langmuir relationship. The vertical strain due to desorption of coal seam degassing can be defined as:

$$\varepsilon_{ds} = \frac{\varepsilon_{max} p_g}{P_L + p_g} \quad (12)$$

where ε_{ds} is the desorption-induced strain, ε_{max} is the maximum strain at infinite pore pressure, p_g is the current gas pressure, and P_L is the pore pressure at which the measured strain is equal to $0.5\varepsilon_{max}$.

Figure 3 coal strain curves at 27°C under different pressures (see online version for colours)



The relationship between the desorption-induced strain and current pore pressure is presented in Figure 3 (Robertson and Christiansen, 2007). Generally, the curves vary widely for different coal quality and gas types. The parameter values in equation (12) can be fitted by Langmuir relationship after the coal samples are tested in laboratory tests.

For a change in pore pressure during the course of gas extraction, the linear desorption-induced strain can be determined by the following relationship:

$$\varepsilon_{ds,t} = \frac{\varepsilon_{max} p_g}{P_L + p_g} - \frac{\varepsilon_{max} p_0}{P_L + p_0} \quad (13)$$

where $\varepsilon_{ds,t}$ is the desorption-induced strain at the current pore pressure after a given time, t , and p_0 is the initial pore pressure in the target coal seam formation.

The desorption-induced compaction, S_{ds} , for a coal seam with thickness H , can be defined as:

$$S_{ds} = \frac{\varepsilon_{\max} P_L}{(P_L + p_g)(P_L + p_0)} \Delta p_f H \quad (14)$$

where $\Delta p_f = p_g - p_0$ is the pressure change.

The total compaction in the geological profile can be calculated as follows:

$$S_{\max} = S_{\text{coal}} + S_{\text{indirect}} + S_{ds} = \sum_{i=1}^N C_{m(i)} H_{(i)} \alpha_{(i)} \Delta p_{f(i)} + \frac{\varepsilon_{\max} P_L}{(P_L + p_g)(P_L + p_0)} \Delta p_f H \quad (15)$$

3 Coupled fluid flow-geomechanical model

During the early stage of depressurisation, the predominant flowing fluid is water, which can be considered as a single phase flow from the coal seam formation to the well. After the large depressurisation, gas desorbs from the coal seams and a continuous gas flow is developed towards the extraction well. This stage is characterised by two-phase flow.

The mathematical model is developed based on the following assumptions:

- 1 the coal and the other layers are assumed to be isotropic and elastic continuum
- 2 the magnitude of deformation is much smaller than the length scale
- 3 the rate of water or gas flow through the layers can be described by the Darcy's law
- 4 gas within the coal seam is ideal and its viscosity is constant under isothermal conditions.

3.1 Governing equation for rock deformation

The strain-displacement relationship of geological units can be defined as:

$$\varepsilon_{ij} = \frac{1}{2} (u_{i,j} + u_{j,i}) \quad (16)$$

where ε_{ij} is the component of total strain, and u_i is the component of displacement.

The equilibrium equation can be written as:

$$\sigma_{ij,j} + f_i = 0 \quad (17)$$

where σ_{ij} is the component of total stress, and f_i is the component of body force.

By consideration of the desorption-induced strain and pore pressure effect, the constitutive relation for the rock can be defined as Fjær et al. (2008):

$$\varepsilon_{ij} = \frac{1}{2G} \sigma_{ij} - \left(\frac{1}{6G} - \frac{1}{9K} \right) \sigma_{kk} \delta_{ij} + \frac{\alpha}{3K} p_f \delta_{ij} + \frac{\varepsilon_{ds}}{3} \delta_{ij} \quad (18)$$

where G is the shear modulus, K is the bulk modulus of rock.

Combing equations (16)–(18), yields the following equation (Zhang et al., 2008):

$$Gu_{i,kk} + \frac{G}{1-2\mu} u_{k,ki} - \alpha p_{f,i} - K \varepsilon_{ds,i} + f_i = 0 \quad (19)$$

Equation (19) is the governing equation for coal seam deformation, where the ε_{ds} can be calculated from equation (12) and the p_f can be solved from the two-phase flow equations discussed as follows,

$$p_f = p_{nw} s_{nw} + p_w s_w$$

where p_{nw} and s_{nw} are the pressure and saturation for the non-wetting fluid respectively, and p_w and s_w are the pressure and saturation for the wetting fluid respectively

3.2 Governing equations of two-phase flow

Two phase flow of water and gas occurs when the pore pressure in the coal seams is lower than the desorption pressure. In the coal seams, the wetting phase is water and the non-wetting phase is gas. The water transport in the coal seam can be described by the mass conservation equation (Comsol, 2013):

$$\frac{\partial(\phi \rho_w s_w)}{\partial t} + \nabla \cdot \left(-\frac{k k_{rw}}{u_w} \rho_w (\nabla p_w + \rho_w g \nabla Y) \right) = f'_w \quad (20)$$

where ϕ is the porosity of coal seam, ρ_w is the water density, s_w is the water saturation, k is the absolute permeability of coal seam, k_{rw} is the relative permeability of coal seam, u_w is the water viscosity, p_w is the pore pressure of water, g is the gravitational acceleration, Y is the coordinate of vertical elevation, and f'_w is the source of water.

For gas phase, the mass conservation equation can be defined as Comsol (2013) and Wang and Peng (2014):

$$\frac{\partial m}{\partial t} + \nabla \cdot \left(-\frac{k k_{mw}}{u_{mw}} \rho_{mw} (\nabla p_{nw} + \rho_{mw} g \nabla Y) \right) = f'_{nw} \quad (21)$$

where k_{mw} is the relative permeability of gas, u_{mw} is the gas viscosity, ρ_{mw} is gas density, p_{nw} is the pore pressure of gas, f'_{nw} is the source of gas, and m is the gas content including free-phase gas, absorbed gas, and the gas diffusion between the coal matrix and the cleats, is defined as:

$$m = \phi \rho_{nw} s_{nw} + \rho_{ga} \rho_c \frac{V_L p^*}{P_L + p^*} + \rho_{ga} \rho_c m_b \quad (22)$$

where s_{nw} is the gas saturation, ρ_{ga} is the gas density at standard condition, ρ_c is the coal density, V_L is the Langmuir volume constant, P_L is Langmuir pressure constant, p^* is the partial gas pressure, $p^* = s_{nw} p_{nw}$, and m_b is the average remaining gas content in the

matrix, $\frac{dm_b}{dt}$ denotes the exchange rate of the gas content between the coal matrix and the cleats.

The gas density can be described by the gas pressure according to the state equation:

$$\begin{cases} \rho_{mw} = \frac{M}{ZRT} p_{mw} = \beta p_{mw} \\ \rho_{ga} = \beta p_a \end{cases} \quad (23)$$

where M is the molecular weight of gas, Z is the gas compressibility factor, R is the gas constant, T is the gas temperature, p_a is the atmosphere pressure.

Therefore, the mass conservation equations of water and gas can be simplified as follows:

$$\begin{cases} \frac{\partial(\phi s_w)}{\partial t} + \nabla \cdot \left(-\frac{kk_{rw}}{u_w} (\nabla p_w + \rho_w g \nabla Y) \right) = \frac{f'_w}{\rho_w} = f_w \\ \frac{\partial}{\partial t} \left(\phi s_{nw} p_{nw} + p_a \rho_c \frac{V_L p^*}{P_L + p^*} \right) + \nabla \cdot \left(-\frac{kk_{rnw}}{u_{nw}} p_{nw} (\nabla p_{nw} + \rho_{nw} g \nabla Y) \right) = \frac{f'_{nw}}{\beta} = f_{nw} \end{cases} \quad (24)$$

The capillary pressure p_c is defined as the difference between the pressure of the non-wetting and wetting phases:

$$p_c = p_{nw} - p_w \quad (25)$$

The available pore space can be completely filled with one fluid at a given time, which relates the effective saturations for each phase:

$$s_{nw} + s_w = 1 \quad (26)$$

The specific capacity of the water, C_p , depends on the changes in the water saturation with respect to the capillary pressure as :

$$C_p = \frac{\partial s_w}{\partial p_c} = \frac{\partial(1-s_{nw})}{\partial p_c} = -\frac{\partial s_{nw}}{\partial p_c} \quad (27)$$

The capillary can be defined as:

$$p_c = p_e \left(\frac{1}{s_w^m} - 1 \right)^{1/n} \quad (28)$$

where p_e is the entry capillary pressure, and is the model parameter.

The van Genuchten-Mualem model is used to build the relative permeability model (Comsol, 2013), which can be expressed as:

$$k_{rw} = s_w^L \left[1 - \left(1 - s_w^m \right)^m \right]^2 \quad (29)$$

$$k_{rmw} = (1 - s_w)^L \left(1 - s_w^m \right)^{2m} \quad (30)$$

where L and m are the parameters of van Genuchten-Mualem model.

By introducing the change of the capillary pressure with saturation in equation (24), the final form of two-phase flow can be defined as:

$$\begin{cases} -\phi C_p \frac{\partial p_w}{\partial t} + \nabla \cdot \left(-\frac{kk_{rw}}{u_w} (\nabla p_w + \rho_w g \nabla Y) \right) = -\phi C_p \frac{\partial p_{nw}}{\partial t} + f_w \\ \phi' (s_{nw} - p_{nw} C_p) \frac{\partial p_{nw}}{\partial t} + \nabla \cdot \left(-\frac{kk_{rmw}}{u_{nw}} p_{nw} (\nabla p_{nw} + \rho_{nw} g \nabla Y) \right) \\ = -\phi' p_{nw} C_p \frac{\partial p_w}{\partial t} - p_a \rho_c \frac{dm_b}{dt} + f_{nw} \end{cases} \quad (31)$$

where ϕ is the desorption modified porosity, $\phi' = \phi + p_a \rho_c \frac{V_L P_L}{(P_L + p^*)^2}$.

The diffusion exchange rate of the gas content can be described as (Chen et al., 2013; Wang and Peng, 2014):

$$\frac{dm_b}{dt} = -\frac{1}{\tau} (m_b - m_e(p_{nw})) \quad (32)$$

where τ is the diffusion time coefficient of the coal matrix, m_e is the gas content at a given time which can be calculated by Langmuir.

By assuming that water saturation s_w is equal to 1.0, the equation (20) is also suitable for the overlying and underlying rock of the coal seam formation.

4 Model comparison

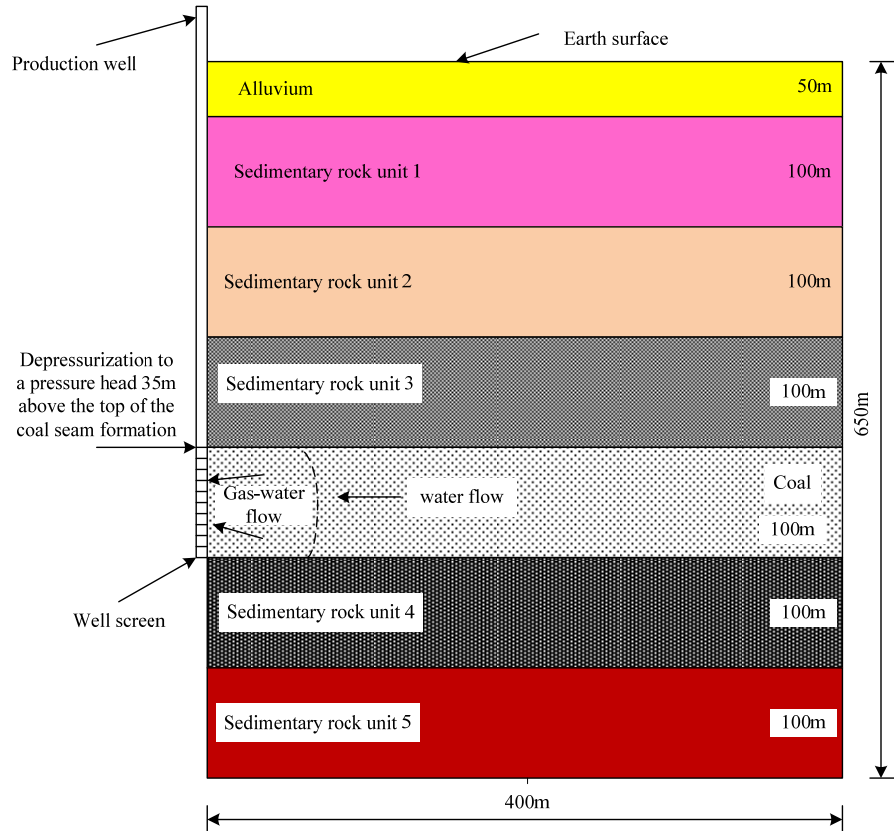
To verify the proposed coupled fluid flow-geomechanical model, two simple comparisons of subsidence induced by gas extraction and desorption-induced strain by degassing are presented, with results of analytical models including the disc-shaped reservoir model and the uniaxial compaction model.

To conduct an analysis of subsidence in coal seam with the numerical model, a conceptual axisymmetric model is established with a well spacing of 800m (it is a common distance in coal seam gas well fields (Australian, 2014)). From the top to the bottom of the model, the strata are alluvium, sedimentary unit 1, sedimentary unit 2, sedimentary unit 3, coal seam, sedimentary unit 4 and sedimentary unit 5, respectively, as shown in Figure 4. The coal bearing formation is located from the depth 350 m to 450 m (correspondingly the thickness is 100 m).

The mechanical and physical properties of the coal bear formation are assumed to be those of the coal, although it is quite possible that the net thickness of the coal seams is only a fraction of the coal bearing formation thickness. Furthermore, we assume dewatering has lowered the groundwater head level to 35m above the CSG bearing formation, which is the typical degree of dewatering required for CSG production. Thus,

a drawdown of the wellbore pressure would occur. We keep dewatering for 10 days, and then fix it to keep degassing. The methane is assumed to be desorpted and diffused from the coal matrix immediately, and controlled mainly by gas Darcy flow rather than by its diffusion in the matrix (Kennon et al., 2010; Seidle and Arri, 1990).

Figure 4 Conceptual model for subsidence prediction in CSG production (see online version for colours)



4.1 Comparison of dewatering effects

In the following, we present an example to illustrate the effects of dewatering on surface subsidence. In this example, the ground profile comprises horizontally layered strata, including two impermeable geological units underlying and overlying the coal bearing formation. In order to make a comparison with analytical models, the coal bearing formation is assumed to have the same mechanical and physical properties as the other formations and the water head difference is 315 m along the coal bearing formation. The stress field is litho static and pore pressure is hydrostatic. The top boundary is as the free surface and the other three boundaries are set as roller condition. The pressure on the top boundary is specified 0 MPa. The wellbore pressure on the coal seam is applied to a

pressure drawdown and the other part of the model is considered impermeable. The geological unit properties are listed in Table 1.

Table 1 Property used in numerical modelling

Geological unit	Compressibility coefficient C_m/MPa^{-1}	Permeability/ m^2	Porosity
Alluvium(saturated)	5.38×10^{-5}	1.19×10^{-15}	0.13
Rock unit 1	5.38×10^{-5}	1.19×10^{-15}	0.13
Rock unit 2	5.38×10^{-5}	0.356×10^{-15}	0.13
Rock unit 3	5.38×10^{-5}	-	-
Coal bearing formation	5.38×10^{-5}	1.19×10^{-15}	0.13
Rock unit 4	5.38×10^{-5}	-	-
Rock unit 5	5.38×10^{-5}	1.19×10^{-16}	0.13

Figure 5 shows the subsidence curves with the change of Poisson's ratio for the two typical analytical models in the case of the same value m_v . The results show that the magnitude of subsidence for the uniaxial model is larger than that for Geerstma's model, in which the far-field boundary of coal seam reservoir is impermeable and the radius R is 400 m. Given that the uniaxial model ignores the lateral extent of the reservoir, the subsidence was the same (i.e., 16.6 mm) for different Poisson's ratios; however the maximum vertical surface deformation for the Geerstma's model was changed with the variation of Poisson's ratio of CSG bearing formation.

Figure 5 Subsidence comparison of uniaxial model and Geerstma's model for different Poisson's ratio: $D/R = 1$, biot coefficient = 1 (see online version for colours)

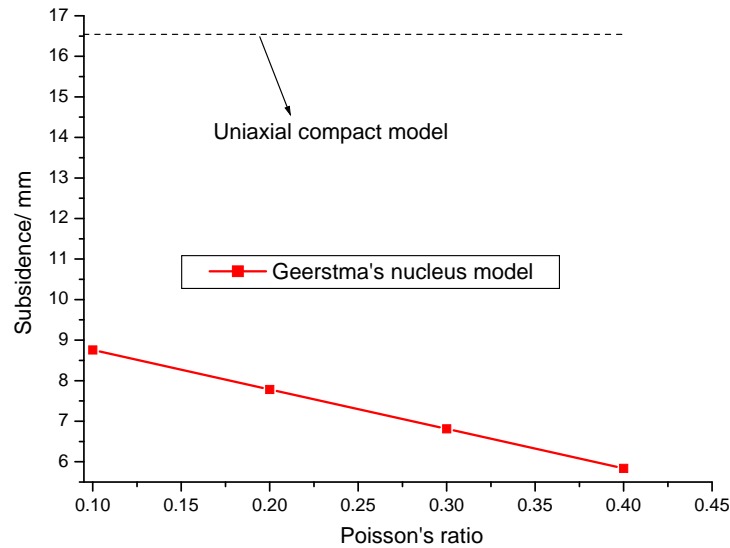
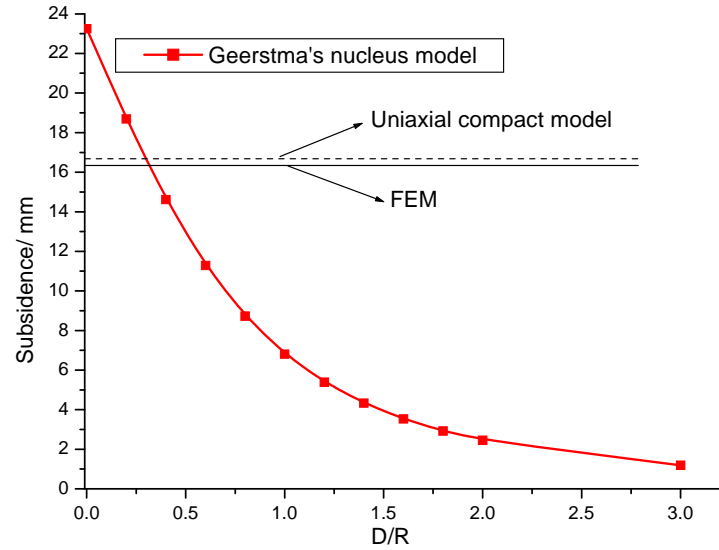


Figure 6 Subsidence comparison of three models for different ratio D/R (see online version for colours)

One of the major controls of subsidence is the ratio D/R of the target reservoir (D and R are the depth and radius of reservoir respectively, as mentioned in Section 2.1). Figure 6 shows the maximum vertical subsidence with the variation of the ratio D/R for the three models (the coupled numerical model, the uniaxial compact model, and the Geerstma's model). One can see that for the extreme state of decreasing the water head 315 m in the whole CSG formation, the results of the uniaxial model are marginally larger than those of the numerical results, and they are both nearly constant. However, the results of the Geerstma's model is not constant, but decreases obviously with the increase of D/R. Due to the same conditions for the well screen (as near field) and the right boundary (as far field), the results demonstrated that it is feasible for the uniaxial model and the coupled numerical model, and is not feasible for the Geerstma's model to calculate subsidence of coal seam extraction in one dimensional condition. Considering that the conventional oil and gas traps are different with the coal seam reservoir, there are more restricted conditions for the Geerstma's model used in the coal seam extraction, such as the shape, impermeable surrounding rock, and the radius of the target reservoir.

4.2 Comparison of degassing effects

Uniaxial compact model is one dimension in the vertical direction ignoring the lateral extent of coal seam formation (Yang et al., 2016). To compare the proposed numerical method with the uniaxial compaction model, a typical conceptual model for one-dimensional desorption-induced deformation is developed, in which the pore pressure change on left boundary (wellbore) is consistent with the right boundary (far field) and this degassing stage is characterised by single-phase gas flow in the coal seam. The same geometrical model as Figure 4 is applied to calculate the desorption-induced

deformation of coal seam formation. The sorption properties of coal seam formation are shown in Table 2.

Table 2 Coalbed sorption properties used in computation

Parameter	Value	Physical meanings
P_L	4.3 MPa	Langmuir pressure of CH ₄ in coal
ε_{max}	0.0078	Langmuir strain at infinite pore pressure
V_L	15 m ³ /t	Langmuir capacity of coal for CH ₄
K_S	27.88 GPa	Bulk modulus of coal grains
s_{w0}	99.99%	Initial water saturation in coal seam
μ_g	1.84×10^{-5} Pa · s	Methane dynamic viscosity
ρ_{ga}	0.717 kg/m ³	Density of methane at standard condition
L	0.50	Genuchten-Mualem model parameter
m	0.65	Genuchten-Mualem model parameter
n	2.80	Genuchten-Mualem model parameter

Source: Australian (2014), Chen et al. (2013)

Figure 7 Desorption-induced strain comparison between analytical and numerical model (see online version for colours)

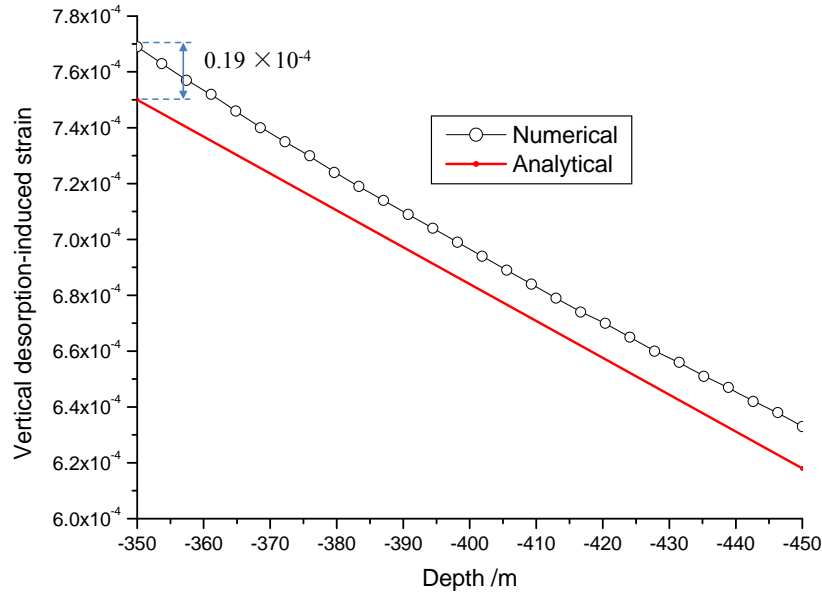
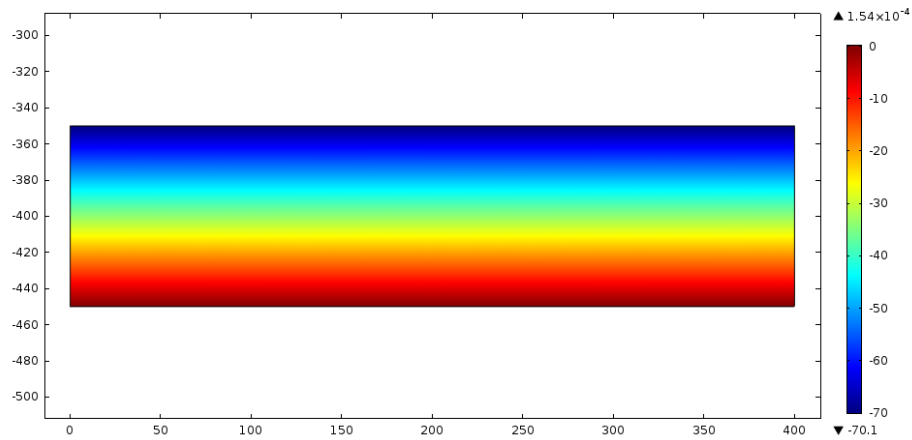


Figure 7 shows the results of the desorption-induced strain with depth for the uniaxial model and the coupled numerical model. One can see that the desorption-induced strains for the uniaxial model are consistent in trend with the numerical results. For comparison, at the top of the coal bearing formation, the maximum strain difference between the analytical and numerical coupled models is 0.19×10^{-4} , with the relative error of 2.47%;

The maximum subsidences for the numerical model and the analytical model are 70.10 mm (as shown in Figure 8) and 68.42 mm [derived from equation (5)] respectively, and the corresponding error is about 2.46%. Although the results are very close for the two models, the uniaxial compact model is limited only in an extreme state when the value of decreased water head is the same in the whole CSG formation (one dimension condition), and ignores the lateral extent of coal seam formation (three dimension condition), thus it may over-estimate the subsidence.

From the above two comparisons, it concludes that the coupled model may be more suitable than analytical models in analysis of subsidence of coal seam gas extraction without the limitation of one dimension condition, geometry of coal seam reservoir and so on.

Figure 8 Deformation contour of numerical simulation (see online version for colours)

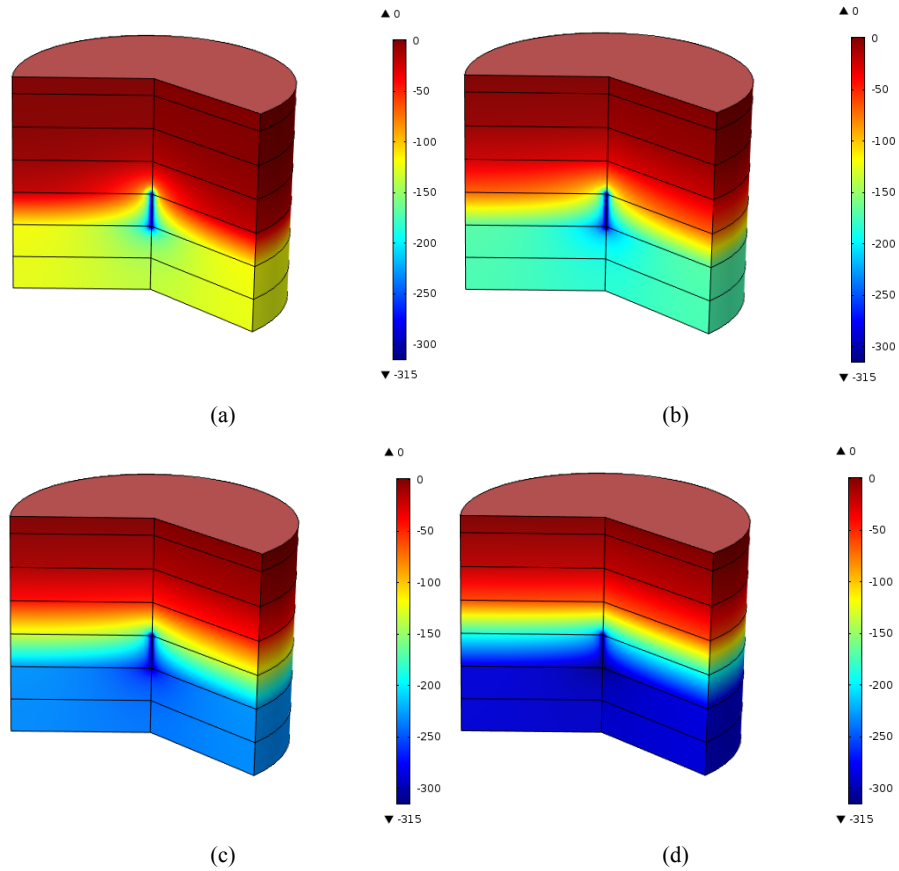


5 Coupled fluid flow-deformation characteristics induced by coal seam gas extraction

According to the conceptual model shown in Figure 4, the deformation and pore pressure evolution of sedimentary layers induced by water and gas withdraw are simulated by the proposed numerical method. In this case, the underlying and overlying layer of coal seam formation is considered as permeable rock, which is consistent with the real engineering condition. The initial condition and boundary conditions are the same with the numerical model in section 4.1. The geomechanical properties of the coal seam are assigned in Tables 1 and 2, and the properties of the other layers are listed in Table 3.

Figure 9 displays the modelling results showing pore pressure reduction over the whole geological units at different time. The pore pressure reduction is greatest near the production well. The pressure head in the coal seam reduces gradually and the extent of the depressurised coal increases with time. The pore pressure reduction across underlying the coal seam formation is larger than that of overlying layer, due to a higher pore pressure gradient between the coal seam and the underlying formation.

Figure 9 Transient pore pressure reduction (water pressure head, m) response to application of drawdown at different times during gas extraction; (a) 500 d, (b) 1,000 d, (c) 2,000 d, (d) 4,000 d (see online version for colours)



As the pumping of groundwater and coal seam gas production, the pore pressure decreases with time. Figure 10 shows the pore pressure distribution at different times in the vicinity of the production well after gas extraction. The pore pressure change mainly is in the target coal seam, overlying and underlying formations, which depend on the permeability of these layers. The pressure/depth gradient steepens with the depth of the coal seam due to the reduction in the vertical permeability with depth.

Figure 11 present the spatial distribution within the coal seam of the change in pressure head, gas content and desorption induced shrinkage strain from their initial states after 500 days of gas production. It can be seen that the difference is significant in the vicinity of the well but diminishes gradually with radial distance.

Table 3 General model parameters of different layers

Property	Alluvium (saturated)	Rock unit 1	Rock unit 2	Rock unit 3	Rock unit 4	Rock unit 5
Young's modulus, GPa	0.2	8	14	20	28	32
Poisson's ratio	0.3	0.25	0.25	0.25	0.25	0.25
Density, kg/m ³	2,100	2,100	2,140	2,140	2,140	2,200
Permeability, × 10 ⁻¹⁵ m ²	1.19	1.19	0.356	0.119	0.119	0.119
Porosity	0.2	0.2	0.16	0.16	0.16	0.16
Biot's coefficient	1	1	1	1	1	1

Source: Australian (2014)

Figure 10 Profiles of pore pressure vs. depth in the vicinity of the coal seam gas extraction well (see online version for colours)

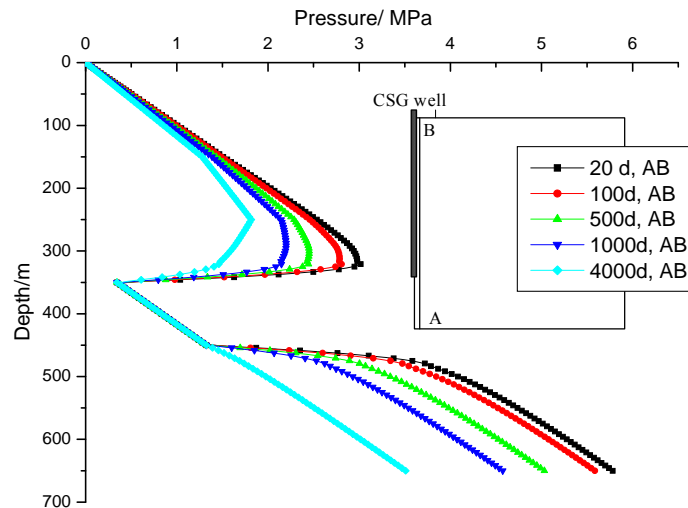
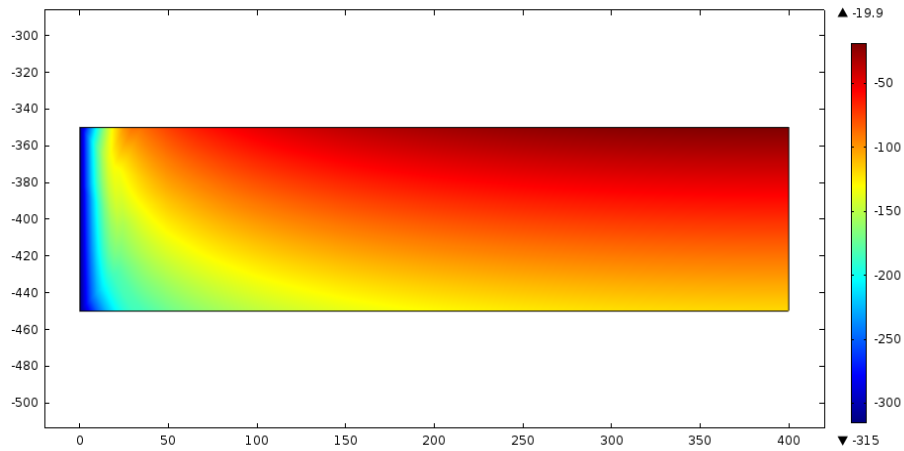


Figure 12 shows the results of horizontal displacement and land subsidence obtained at 500 days after the inception of gas extraction. The maximum subsidence always occurs near the well, while the maximum horizontal displacements occur far away from the injection well. The maximum subsidence is 3.236 cm at 500 days, and the ratio of maximum subsidence over maximum horizontal displacement is about 39. Because the far right edge of the model represents an impermeable symmetry line between the two production wells spaced at 800m, the location of the maximum displacement does not change over time, but the magnitude of displacement increases over time.

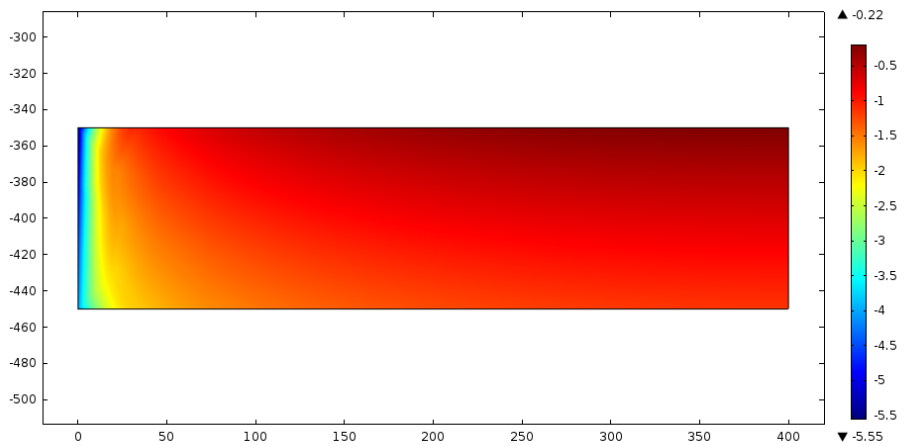
The settlement (vertical displacement) in the vicinity of the well throughout the depth is shown in Figure 13. It can be seen that the settlement of rocks confined coal seam gradually increases with time in short-term depressurising, meanwhile, heave appears in underlying rock of coal seam formation, which is 'rock-arch effect' that influenced by the abrupt pressure change and the difference of permeability between overlying layer and coal seam formation. Pressure drop funnel around the gas extraction well is formed after

coal seam depressurisation with uneven settlement around the coal seam well. For long-term gas extraction, the settlement is mainly determined by the coal seam formation and underlying layers, and the settlement of other overlying layers can not be neglected for the compaction effect.

Figure 11 The spatial distribution of the change in pressure head, gas content and desorption strain from their initial states at 500 days; (a) Change in pressure head (m), (b) Change in gas content (m^3/tonne), (c) Change in desorption strain (see online version for colours)



(a)



(b)

Figure 11 The spatial distribution of the change in pressure head, gas content and desorption strain from their initial states at 500 days; (a) Change in pressure head (m), (b) Change in gas content (m^3/tonne), (c) Change in desorption strain (continued) (see online version for colours)

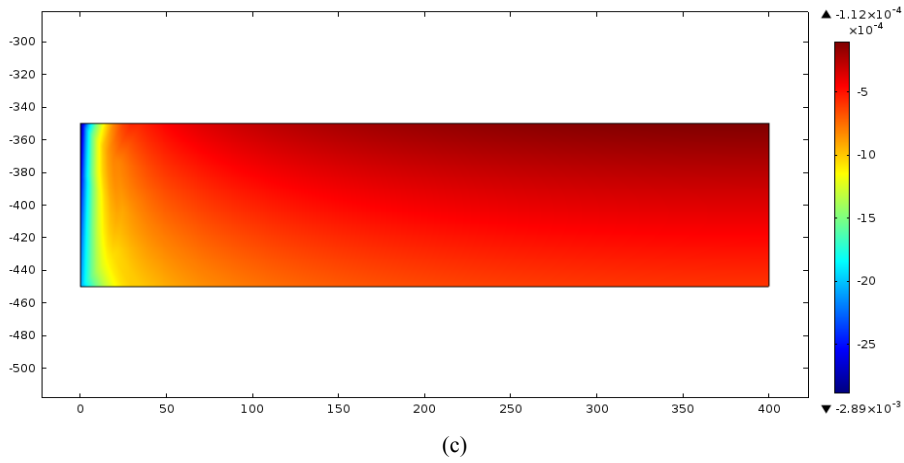


Figure 12 Horizontal displacement and land subsidence curves as a function of radial distance from the injection well at 500 days; (a) Horizontal deformation, (b) Land subsidence

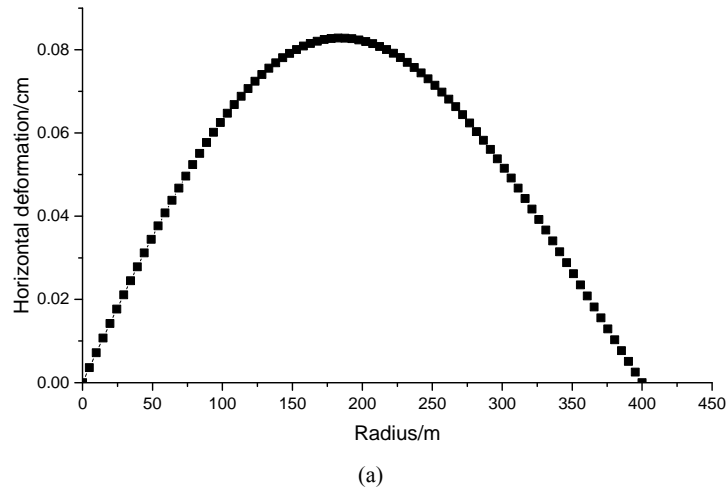
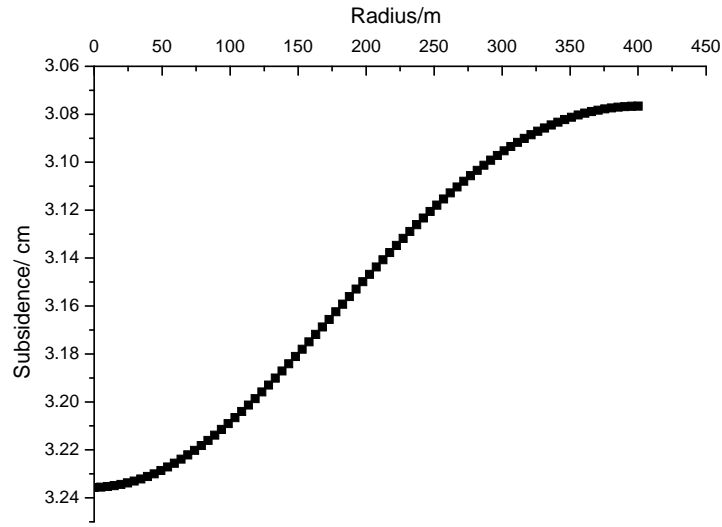
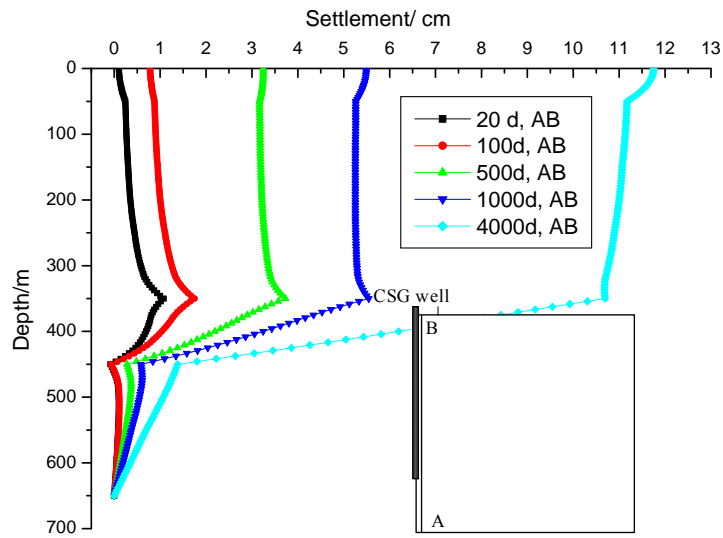


Figure 12 Horizontal displacement and land subsidence curves as a function of radial distance from the injection well at 500 days; (a) Horizontal deformation, (b) Land subsidence (continued)



(b)

Figure 13 Profiles of settlement vs. depth for different times from beginning of well production (see online version for colours)



6 Conclusions

This paper presents some comparisons of a novel coupled hydro-mechanical model with typical analytical models in subsidence of coal seam gas extraction. By comparison of dewatering and degassing effects in coal seam formation, the following conclusions can be made:

For the typical analytical models, the disc-shaped reservoir model disregards the permeability of confining layer of coal seam and is subject to more restricted conditions such as the geometry of coal seam reservoir. The uniaxial compact model is limited to one dimension condition, ignoring the lateral extent of coal seam formation, so they cannot estimate the potential pore pressure distribution and reflect the realistic production.

For the coupled fluid flow-geomechanical model, it can describe the transport properties of coal seam, including water flow, gas flow and desorption, rock deformation, resulting in realistically predicting land subsidence due to coal seam gas extraction.

The coupled multi-physical processes involved in the coal seam gas extraction are not completely understood, especially the permeability evolution of coal seam by mechanical and desorbed effects. Further study is needed to fully comprehend the process.

Acknowledgements

The authors gratefully acknowledge the support of the National Natural Science Foundation of China (Grant Nos. 51379007, 41130742, 51678066), the support of the Chinese Fundamental Research (973) Program through the Grant No. 2013CB036006 and the support of the Open Research Fund of State Key Laboratory of Geomechanics and Geotechnical Engineering (Grant No. Z013007), the Oil and Gas Reservoir Geology and Exploitation (Grant No. PLN1507).

References

- Anderssohn, J., Motagh, M., Walter, T.R., Rosenau, M., Kaufmann, H. and Oncken, O. (2009) 'Surface deformation time series and source modeling for a volcanic complex system based on satellite wide swath and image mode interferometry: the Lazufre system, central Andes', *Remote Sensing of Environment*, Vol. 113, No. 10, pp.2062–2075.
- Australian G (2014) *Background Review: Subsidence from Coal Seam Gas Extraction in Australia*, Australian Government Department of the Environment, Canberra.
- Basu, A., Boyd, M.J. and McConchie, P. (1988) 'Numerical modelling of two phase flow of gas and water during drainage of a coal seam', *International Journal of Mine Water*, Vol. 7, No. 4, pp.27–42.
- Chen, D., Pan, Z.J., Liu, J.S., Connell, L.D. (2013) 'An improved relative permeability model for coal reservoirs', *International Journal of Coal Geology*, Vols. 109–110, No. 2, pp.45–57.
- Comsol, L. (2013) 'COMSOL Multiphysics® Version 4'.
- Coussy, O., Pereira, J.M. and Vaunat, J. (2010) 'Revisiting the thermodynamics of hardening plasticity for unsaturated soils', *Computers and Geotechnics*, Vol. 37, No. 1, pp.207–215.
- Du, J. and Olson, J.E. (2001) 'A poroelastic reservoir model for predicting subsidence and mapping subsurface pressure fronts', *Journal of Petroleum Science and Engineering*, Vol. 30, Nos. 3–4, pp.181–197.

- Fjær, E., Holt, R.M., Horsrud, P., Raaen, A.M. and Risnes, R. (2008) 'Chapter 3 Geological aspects of petroleum related rock mechanics', *Developments in Petroleum Science*, Vol. 53, No. 7, pp.103–133
- Gambolati, G., Ferronato, M., Teatini, P., Deidda, R. and Lecca, G. (2001) 'Finite element analysis of land subsidence above depleted reservoirs with pore pressure gradient and total stress formulations', *International Journal for Numerical and Analytical Methods in Geomechanics*, Vol. 25, No. 4, pp.307–327.
- Geertsma, J. (1973) 'Land subsidence above compacting oil and gas reservoirs', *Journal of Petroleum Technology*, Vol. 25, No. 6, pp.734–744.
- Kennon, S.R., Nair, N., Mccracken, A. (2010) *Methods of Modeling Flow of Gas Within A Reservoir*, United States Patent Application, 20100250215.
- Moghaddam, N.F., Samsonov, S.V., Rüdiger, C., Walker, J.P., Hall, W.D.M. (2016) 'Multi-temporal SAR observations of the Surat Basin in Australia for deformation scenario evaluation associated with man-made interactions', *Environmental Earth Sciences*, Vol. 75, No. 4, pp.1–16.
- Ramirez, A. and Foxall, W. (2014) 'Stochastic inversion of InSAR data to assess the probability of pressure penetration into the lower caprock at in Salah', *International Journal of Greenhouse Gas Control*, Vol. 27, No. 27, pp.42–58.
- Robertson, E.P. and Christiansen, R.L. (2007) 'Modeling permeability in coal using sorption-induced strain data', *SPE Reservoir Evaluation and Engineering*, Vol. 10, No. 3, pp.260–269.
- Sambridge, M. (1999a) 'Geophysical inversion with a neighbourhood algorithm – I. Searching a parameter space', *Geophysical Journal International*, Vol. 138, No. 2, pp.479–494.
- Sambridge, M. (1999b) 'Geophysical inversion with a neighbourhood algorithm – II. Appraising the ensemble', *Geophysical Journal International*, Vol. 138, No. 3, pp.727–746.
- Seidle, J.P. and Arri, L.E. (1990) *Use of Conventional Reservoir Models for Coal Bed Methane Simulation*, Society of Petroleum Engineers.
- Vandamme, M., Brochard, L., Lecampion, B. and Coussy, O. (2010) 'Adsorption and strain: the CO₂-induced swelling of coal', *Journal of the Mechanics and Physics of Solids*, Vol. 58, No. 10, pp.1489–1505.
- Vasco, D.W., Rucci, A., Ferretti, A., Novali, F., Bissell, R.C., Ringrose, P.S., Mathieson, A.S. and Wright, I.W. (2009) 'Satellite-based measurements of surface deformation reveal fluid flow associated with the geological storage of carbon dioxide', *Geophysical Research Letters*, Vol. 37, No. 3, pp.174–180.
- Wang, J.G. and Peng, Y. (2014) 'Numerical modeling for the combined effects of two-phase flow, deformation, gas diffusion and CO₂ sorption on caprock sealing efficiency', *Journal of Geochemical Exploration*, Vol. 144, Part A, pp.154–167.
- Wu, Y., Liu, J., Elsworth, D., Chen, Z., Connell, L., Pan, Z. (2010) 'Dual poroelastic response of a coal seam to CO₂ injection', *International Journal of Greenhouse Gas Control*, Vol. 4, No. 4, pp.668–678.
- Yang, D.S, Qi, X.Y., Chen, W.Z., Wang, S. and Dai, F. (2016) 'Numerical investigation on the coupled gas-solid behavior of coal using an improved anisotropic permeability model', *Journal of Natural Gas Science Engineering*, Vol. 34, pp.226–235.
- Zhang, H., Liu, J. and Elsworth, D. (2008) 'How sorption-induced matrix deformation affects gas flow in coal seams: a new FE model', *International Journal of Rock Mechanics & Mining Sciences*, Vol. 45, No. 8, pp.1226–1236.
- Zhu, W., Zhang, Q., Ding, X.L., Zhao, C., Yang, C., Qu, F., Qu, W. (2014) 'Landslide monitoring by combining of CR-InSAR and GPS techniques', *Advances in Space Research*, Vol. 53, No. 3, pp.430–439.
- Zhu, W.C., Liu, J., Sheng, J.C. and Elsworth, D. (2007) 'Analysis of coupled gas flow and deformation process with desorption and Klinkenberg effects in coal seams', *International Journal of Rock Mechanics and Mining Sciences*, Vol. 44, No. 7, pp.971–980.